

Analysis of *Fermi*-LAT data from Tucana-II: Possible constraints on the Dark Matter models

Pooja Bhattacharjee^{1,2,*}, Sayan Biswas^{3,†}, Pratik Majumdar^{4,‡} and Partha S. Joarder^{1,2§}

¹ Department of Physics, Bose Institute, 93/1 A.P.C. Road, Kolkata 700009, India

² Centre for Astroparticle Physics and Space Science, Bose Institute, Block EN, Sector V, Salt Lake, Kolkata 700091, India

³ Raman Research Institute, C.V. Raman Avenue, Sadashivanagar, Bangalore, Karnataka 560080, India and

⁴ Saha Institute of Nuclear Physics, HBNI, 1/AF, Bidhannagar, Kolkata 700064, India

Tucana-II (Tuc-II), a recently discovered and confirmed Ultra Faint Dwarf Spheroidal galaxy, has a high mass to light ratio as well as a large line-of-sight stellar velocity dispersion, thus making it an ideal candidate for an indirect dark matter search. In this paper, we have analyzed nine years of γ -ray data obtained from the *Fermi*-LAT instrument in the direction of Tuc-II. The fact that no statistically significant γ -ray excess over the background of Tuc-II have been detected from the location of this galaxy. It called for an estimation of the 95% confidence level upper limit of the possible velocity weighted self-annihilation cross-section of the dark matter particles (WIMPs) within Tuc-II by fitting the observed γ -ray flux with the DMFit function. The estimated upper limits of the cross-sections are then compared with similar upper limits of the cross-sections determined by us in three other dwarf galaxies that are considered earlier to be the good dark matter candidates in the literature. We have also compared our results with the cross-sections obtained in various popular theoretical models of the WIMPs to find that our results impose reasonable constraints on the parameter spaces of those models. In the concluding section, we compared our results with the similar results obtained from a combined dSph analysis by the *Fermi*-LAT collaboration as well as the results obtained from the studies of dark matter in the dwarf galaxies by the major ground-based Cherenkov experiments.

Keywords: dark matter, WIMP, ultra faint dwarf spheroidal galaxy, indirect detection.

1. INTRODUCTION

The astrophysical and cosmological observations (e.g., [1, 2]) strongly suggest that some kind of non-luminous and non-baryonic matter, namely the Dark Matter (DM), constitutes almost 75% of the total matter density of the Universe. Regarding the physical nature of such DM, cosmological N-body simulations (e.g., [3, 4]) usually favor a cold DM (CDM) scenario to explain the formation of the large scale structure of the Universe. In addition, the extension of the Standard Model (SM) of particle physics predict that CDM could possibly be consisted of some form of massive, non-baryonic and neutrally charged particles, namely weakly interacting massive particles (WIMPs). WIMPs self pair annihilation (with their masses lying in the range of a few tens of GeV to a few hundreds of TeV) explains the thermal relic abundances (i.e. $\langle \sigma v \rangle \approx 3 \times 10^{-26} \text{ cm}^3 \text{ s}^{-1}$) and are consistent with the currently observed mass density of CDM; e.g., [5–7]. Such pair-annihilation of the WIMPs may be one of the excellent source of indirect dark matter search [5].

DM pair-annihilation rate and the resulting flux of γ -photons are likely to be proportional to the square of the DM density. The dwarf Spheroidal satellite galaxies (dSph) of the Milky Way (MW) that are the densest DM regions in the galactic halo [8], usually lie away from the direction of the central region of the galaxy. Those dSphs are not too far ($\sim (20 - 200)$ kpc) from the earth [9] and they have low content of gas and dust [10], therefore, making them the potentially excellent targets for an indirect search of DM through the detection of the high energy γ -rays arising from the WIMP annihilations [5]. Over about a decade from now, the Sloan Digital Sky Survey (SDSS)[11, 12], the Panoramic Survey Telescope and Rapid Response System (Pan-STARRS) [13–15], the Dark Energy Survey (DES) [16–19] experiment and certain other surveys by using the Dark Energy Camera at Cerro Tololo [20, 21] have discovered a new class of dSphs, namely the Ultra Faint Dwarf galaxies (UFDs) that have extremely low stellar contents and

*pooja.bhattacharjee@jcbose.ac.in

†sayan@rri.res.in

‡pratik.majumdar@saha.ac.in

§partha@jcbose.ac.in

densities. The UFDs are dominated by old ($\gtrsim 12$ Gyr) stellar populations with large radial velocities that possibly indicate the existence of substantial DM components in those UFDs [22]. With their inferred mass-to-light ratios reaching upto $\sim 3000 M_{\odot}/L_{\odot}$, the UFDs are, therefore, considered to be the best tracers of early DM sub-halos in the Universe as predicted by the Λ CDM cosmological models [23]. Recently, a joint DES-*Fermi*-LAT collaboration [24] has examined the γ -ray signatures of the WIMP pair-annihilations from about 45 UFDs with an aim of re-examining the constraints imposed on various theoretical WIMP models by an earlier analysis [25] of the γ -ray data from 15 confirmed dSphs performed by the *Fermi*-collaboration. At present, two new sky survey programs, namely the Large Synoptic Survey Telescope (LSST) and the Wide-Field Infrared Survey Telescope, are being undertaken/planned to search for more UFD/dSph candidates in the galactic halo and in its neighborhood for a comprehensive study of the DM in the Universe [26].

Motivated by such increasing interest in the indirect search for DM in the UFDs/dSphs, earlier, we (see Ref. [27]; referred hereafter as Paper I) undertook a task of analyzing almost seven years of high energy γ -ray data collected by the *Fermi*-Large Area Telescope (*Fermi*-LAT; sometimes referred simply as the ‘LAT’) in the direction of the particular UFD, namely Triangulum-II (Tri-II), which was first investigated by the PAN-STARs 3π program [15]. In that paper, we derived the 95% confidence level (C.L.) upper limit of photon fluxes (above 100 MeV) as well as the upper limit of $\langle \sigma v \rangle$, as a function of the WIMP mass (m_{DM}), for Tri-II for several important WIMP pair-annihilation channels to compare those cross-sections with the ones obtained from a number of theoretical WIMP models. In Paper I, we found that, the constraints on the parameter values of various popular WIMP models, as imposed by the LAT-Data from Tri-II, are stronger than the ones imposed by the *Fermi*-data from UMi, which was considered in Ref. [5] to be one of the best candidates for DM search amongst the dSphs.

In the present paper, we focus our attention to a recently discovered dwarf satellite, namely Tucana-II (Tuc-II; DES J2251.2-5836) [17, 18] that has already been confirmed to be an UFD (and not a part of any globular cluster) in Ref. [28], principally because of its large projected half light radius, the large velocity dispersion of its member stars, its luminosity-metallicity relation and also because of its large dynamical mass to light ratio, all of which conform to the well-established values of the dwarf galaxies [28–32]. Tuc-II may, as well, be a member of the Magellanic group as it is only about 19 kpc away from the Large Magellanic Cloud (LMC) and about 37 kpc away from the Small Magellanic Cloud (SMC) [17]. The outer region of Tuc-II appears to be in elongated and distorted shape but the observational noise could, as well, be the reason for such a distortion [33, 34]. Considering various observationally inferred parameter values of Tuc II, Walker et al. (2016; [28]) had suggested that this UFD may not exhibit one of the strongest DM annihilation signal, but may contribute meaningfully to the analysis of stacked data from multiple sources including Tuc-II. To the best of our knowledge, a *Fermi*-LAT data analysis of the γ -ray signals from Tuc-II, either individually or as a member of a group of a number of UFDs, with the purpose of constraining the parameters of various theoretical DM models, remains hitherto undone. In this paper, we, plan to perform such a data analysis of Tuc II alone to see whether it constrains the parameter space of the popular DM models and how those constraints compare to the ones obtained from the modeling of Tri-II and of UMi in our earlier analysis [27]. Here, we also compare our results on Tuc-II with the ones obtained from the recent DES-discovered UFD, namely Reticulum-II (Ret-II) [18, 35], the *Fermi*-LAT data analysis of which has already been done in Refs. [24, 36] that seem to exhibit small excess of γ -ray signal of some significance over the background of Ret-II, thus making Ret-II an attractive source to search for the annihilation signals of DM [36]. Our comparison, presented in this paper, have again shown that the constraints imposed by Tuc-II on the popular WIMP models in all the relevant annihilation channels are stronger than the ones obtained in the case of Ret-II. For the sake of such study, we here assume a perfect spherical symmetry for Tuc-II and further assume Tuc-II to be in dynamic equilibrium with a negligible contribution to its significantly large, observed line-of-sight stellar velocity dispersion from the possible binary stellar motions in Tuc-II, thus assuming that the gravitational potential of Tuc-II is entirely dominated by DM [28].

The paper is organized along the following line. After stating the observed properties of Tuc-II (in subsection 2.1) that are relevant for our study, we briefly describe the procedure for the analysis of *Fermi*-LAT data from the direction of Tuc-II in subsection 2.2. In subsection 2.3, we estimate the possible upper limits of the γ -ray flux from Tuc-II by fitting Tuc-II with power law spectral models with five different power indices. In subsection 3.1, we employ the NFW density profile to model the DM density in Tuc-II. In that subsection, we also estimate the J -factor for the possible γ -ray flux arising from the WIMP pair-annihilation in Tuc-II. In subsection 3.2, we determine the possible upper limit of the γ -ray flux from Tuc-II by using the DMfit Monte Carlo (MC) simulation package [37]. There, we also calculate the possible upper limits of the velocity-averaged pair-annihilation cross-section $\langle \sigma v \rangle$ of the WIMPs for several important pair-annihilation channels by using DMfit to compare those cross-sections with the ones obtained from various theoretical WIMP models. Comparisons of the results from Tuc-II, first with the ones obtained from Tri-II and UMi in Paper I and then with the results obtained from Ret-II (as in Ref. [24]), are also presented in subsection 3.2 of this paper. Finally, a brief discussion of our results presented here *vis-a-vis* the results obtained from UFDs/dSphs with the *Fermi*-LAT and with various ground-based Cherenkov-experiments at higher energies is presented in the concluding section 4.

2. ANALYSIS OF TUC-II

2.1. The relevant observed properties of Tuc-II

A spectroscopic study of a number of stars in the direction of Tuc II was undertaken by Walker et al. [28] by the use of the Michigan Magellan Fibre System (M2FS). This study, along with the previous photometric results on Tuc-II [18, 38], could identify eight probable member stars of Tuc-II that were sufficiently well-resolved to determine an internal velocity dispersion $\sigma_v = 8.6^{+4.4}_{-2.7}$ km s⁻¹ about a mean velocity of $-129.1^{+3.5}_{-3.5}$ km s⁻¹ in the solar rest frame. These and the other important physical properties of Tuc-II that have either been directly observed or have been inferred from the observations of Tuc-II by the authors of Refs. [18, 28], are tabulated in Table-I for later reference.

TABLE I: Properties of Tuc-II

Property	Value	Reference
Galactic latitude	328.08.63°	[18]
Galactic longitude	-52.3248°	[18]
Heliocentric distance ([D])	57 ⁺⁵ ₋₅ kpc	[18]
Metallicity ([Fe/H])	< 0.4	[28]
2D projected half light radius (R_h)	165 ⁺²⁸ ₋₁₉ pc	[18]
Maximum galactocentric angular distance in the sample of the observed member stars in Tuc-II, as measured from the observer's position ($[\theta_{\max}]$)	1°	[36, 39]
Square-root of the luminosity-weighted square of the line-of-sight stellar velocity dispersion (σ_v)	8.6 ^{+4.4} _{-2.7} km s ⁻¹	[28]
Mass within the 2D projected half-light radius ($\frac{M_{1/2}}{M_\odot}$)	2.7 ^{+3.1} _{-1.3} × 10 ⁶	[28]
Dynamical mass-to-light ratio ($((M/L_v)_{1/2})$)	1913 ⁺²²³⁴ ₋₉₅₀ M _⊙ L _⊙ ⁻¹	[28]
The J -factor at θ_{\max}	0.457 × 10 ²⁰ Gev ² cm ⁻⁵	

In Table I, M_\odot and L_\odot indicate the mass and the total luminosity of the Sun, respectively. Definitions of various other quantities displayed in Table I are given in [28, 36]; also see Refs.[39–41]. In the subsection 3.1, we will use some of the parameters of Tuc-II enlisted in Table-I to evaluate the so-called J -factor, and hence the γ -ray flux arising from DM annihilation in Tuc-II.

2.2. The *Fermi*-LAT data analysis of Tuc-II

The *Fermi*-LAT is a γ -ray space-based detector that scans the whole sky every 3 hour for an efficient study of the γ -ray sky in an energy range from about 20 MeV to 500 GeV. In this paper, we have used the recent version v10r0p5¹ of the *Fermi* ScienceTools for the analysis of γ -ray data from Tuc-II. The above version allows us to use the pre-processed PASS 8 dataset of event class 128 that makes use of an improved instrument response function (IRF)

¹ <https://fermi.gsfc.nasa.gov/ssc/data/analysis/software/>

P8R2_SOURCE_V6² of the LAT. Here, we have extracted nearly nine years (i.e. from 2008-05-04 to 2015-05-22) of LAT data in 100 MeV to 300 GeV reconstructed energy range within a 20° radius of interest (ROI) centered on the location of Tuc-II. As in Paper I, we have applied a zenith angle cut at 90° ³ and we have selected the good time intervals (GTIs) by using the ‘gtmktime’ filter [5]. Next, we perform the binned likelihood analysis of our extracted dataset with the ‘gtlike’ tool [42, 43] by following the instructions⁴ given in the `ScienceTools`. In this analysis, the spectral parameters of all the *Fermi*-3FGL sources [44] within 5° of the ROI, as well as, the normalization parameters of the two background models⁵ (i.e. `gll_iem_v06.fits` and `iso_P8R2_SOURCE_V6_v06.txt`) have been left free during the model fitting procedure. The rest of the sources in the ROI have been kept fixed at their values given in the 3FGL catalog. As the LAT could not detect significant γ -emission from the particular location of Tuc-II, we included Tuc-II in our source model along with the usual 3FGL sources in its neighborhood. In the following, we first model Tuc-II as a source having a power-law spectrum with each of the five different spectral indices and later we go over to fit the γ -ray spectrum arising from the (assumed) DM-dominated Tuc-II with a MC-simulated DM self-annihilation spectrum generated by the use of the DMfit simulation tool-kit [37].

2.3. Results of the power-law modeling

In Fig. 1(a), we display the spectral fit of all the sources within the aforesaid ROI, along with the isotropic background component and the galactic diffuse background component, in the case of Tuc-II and its neighborhood in this paper also. Similarly, Fig. 1(b) displays the corresponding residual plot for all the above sources in the given ROI. The horizontal axes in both these figures indicate the reconstructed energy E of the γ -photons within the chosen range. While the above figures display only the results for modeling Tuc-II with a spectral index $\Gamma = 2$ alone, we have actually repeated this spectral fitting procedure for each of the other values of the spectral index, namely $\Gamma = 1, 1.8, 2.2$ and 2.4 , as well. The best-fitted values of the normalization constant (N_0) and the Test Statistics (TS) obtained from Tuc-II for each of those spectral indices are displayed in Table-II. It is evident from the TS values that the LAT could not detect excess γ -emission of any significance from the direction of Tuc-II. Hence, we calculate the flux upper limit from Tuc-II over the entire reconstructed energy range (0.1 – 300) GeV, chosen in this paper, by the profile likelihood method [45, 46]. Next, we have also applied the Bayesian method, implemented already in the `ScienceTools` [5], to obtain a more accurate γ -ray flux upper limit with 95% confidence level (C.L.) from Tuc-II. Such upper limits are displayed in Table-III for each of the model power-law spectrum considered above. In Table-III, we note that, the 95% C.L. γ -flux upper limit for $\Gamma = 1$ is almost an order of magnitude lower than the one corresponding to $\Gamma = 2.4$. This result is consistent with our results for Tri-II in Paper-I [27]. It is also consistent with the earlier results [5] obtained from a similar analysis of γ -ray data from a number of dSphs.

TABLE II: Best-fitted normalization parameters and the TS values obtained from the spectral fittings of the γ -ray flux from Tuc-II with five different spectral indices (Γ) as indicated in the Table.

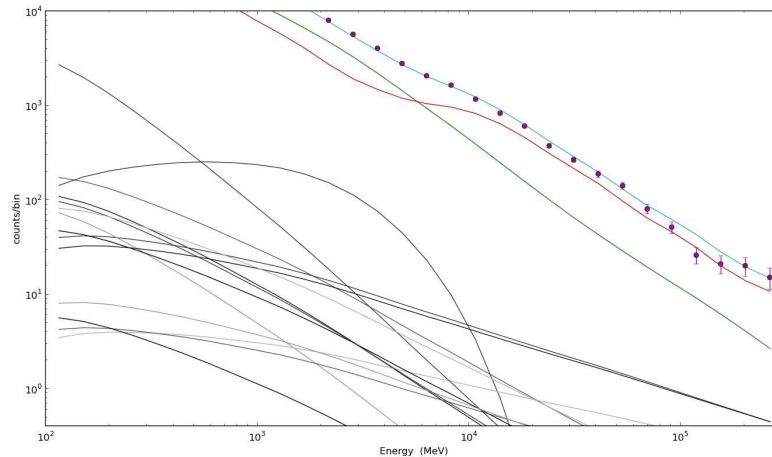
Spectral Index (Γ)	$N_0 \times 10^{-5}$	Test Statistic (TS) value
1	$(1.20 \pm 1.97) \times 10^{-9}$	0.58
1.8	$(5.57 \pm 6.89) \times 10^{-9}$	0.002
2	$(5.06 \pm 6.31) \times 10^{-8}$	-0.13
2.2	$(1.08 \pm 3.32) \times 10^{-7}$	-0.60
2.4	$(3.04 \pm 4.84) \times 10^{-7}$	-0.57

² https://fermi.gsfc.nasa.gov/ssc/data/analysis/documentation/Pass8_usage.html

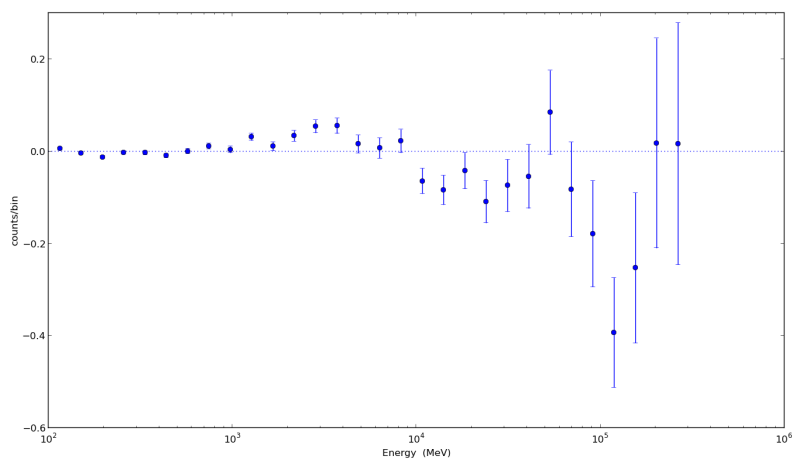
³ <https://fermi.gsfc.nasa.gov/ssc/data/analysis/scitools/help/gtselect.txt>

⁴ https://fermi.gsfc.nasa.gov/ssc/data/analysis/scitools/binned_likelihood_tutorial.html

⁵ <https://fermi.gsfc.nasa.gov/ssc/data/access/lat/BackgroundModels.html>



(a)



(b)

FIG. 1: Spectral fit to the counts (Fig. 1(a)) and the corresponding residual plot (Fig. 1(b)) are displayed for all the sources within the chosen ROI centred on Tuc-II, in which the power-law source-spectral index of Tuc-II is taken as $\Gamma = 2$. In Fig. 1(a), the sky curve displays the best-fit total spectrum, along with the corresponding LAT-observed data points (in magenta); the green and the red curves display the galactic diffuse background and the isotropic background component, respectively. The rest of the curves correspond to various point sources other than Tuc-II, lying within the ROI that are not distinctly labelled in Fig. 1(a).

TABLE III: 95% C.L. γ -ray flux upper limit obtained from the power-law spectral modelings of Tuc-II with five different spectral indices (Γ) as indicated in the Table.

Spectral Index (Γ)	Flux upper limits in 95% C.L. ($\text{cm}^{-2} \text{s}^{-1}$)
1	6.08×10^{-11}
1.8	3.28×10^{-10}
2	4.05×10^{-10}
2.2	4.23×10^{-10}
2.4	4.61×10^{-10}

3. THE γ -RAY SIGNATURE OF THE WIMP-ANNIHILATIONS IN TUC-II AND THE CONSTRAINTS ON THE DM MODELS

3.1. Estimation of the flux of γ -rays from Tuc-II

The expression for the differential photon flux, arising from WIMP pair-annihilations, in a DM source subtending a solid angle $\Delta\Omega$ at the observer's location is known (e.g., [5, 47]) to be

$$\phi_{\text{WIMP}}(E, \Delta\Omega) = \Phi^{pp}(E) \times J(\Delta\Omega), \quad (1)$$

in which, $\Phi^{pp}(E)$, with the photon energy E , is the *Particle physics factor*; whereas, $J(\Delta\Omega)$ in Eq. (1) is the *Astrophysical factor* or the *J-factor*. In the following, we reproduce brief descriptions of these factors for the sake of completeness.

3.1.1. Particle physics factor

The expression for the particle physics factor that provides information regarding the properties of the initial and the final state particles in various possible WIMP pair-annihilation channels, is given by [5]

$$\Phi^{pp}(E) = \frac{\langle \sigma v \rangle}{8\pi m_{\text{WIMP}}^2} \sum_f \frac{dN_f}{dE} B_f. \quad (2)$$

In Eq. (2), $\langle \sigma v \rangle$ denotes the thermally averaged product of the relative velocity between the WIMPs and their pair-annihilation cross-section [5]; whereas, $\frac{dN_f}{dE}$ and B_f denotes the differential photon spectrum per DM annihilation and the branching ratio of a particular WIMP pair annihilation final state “ f ”, respectively.

3.1.2. Astrophysical factor (*J-factor*)

The expression for the *J-factor* in Eq. (1) that contains the information regarding the astrophysical properties of the potential DM source (i.e., Tuc-II in the context of this paper), takes the form [5]:

$$J(\Delta\Omega) = J(\lambda, \theta) = 2\pi \int_0^{\theta_{\text{max}}} \int_{\lambda_{\text{min}}}^{\lambda_{\text{max}}} \rho^2(\sqrt{\lambda^2 + d^2 - 2\lambda d \cos \theta}) d\lambda d\theta, \quad (3)$$

where, $\rho(r)$ is the radial distribution of the DM mass-density in Tuc-II. In Eq. (3), λ is the line-of-sight (l.o.s) distance, d is the heliocentric distance of the centre of Tuc-II and θ is angle between the l.o.s and the centre of Tuc-II, respectively. In our analysis, we have considered the Navarro-Frenk-White (NFW) density profile [48] for modeling the DM distribution in Tuc-II.

Like in Paper-I, we use a simple analytical formula for the evaluation of the *J-factor* in this paper also. This approximate formula was originally provided in Ref. [39] from the solutions of the spherical Jeans' equation in the particular cases of the spherical or the nearly spherical dwarf satellites at sufficiently large distances from the Sun. This formula is given as

$$J \approx \frac{25}{8G^2} \frac{\sigma_v^4 \theta_{\text{max}}}{dR_h^2}. \quad (4)$$

In Eq. (4), $\theta_{\text{max}} = \arcsin(r_{\text{max}}/D)$; r_{max} is an estimate of the maximum galactocentric distance in the sample of the observed member stars [39] in Tuc-II. The value of θ_{max} and those of the other constants required in Eq. (4) for a numerical estimation of J for Tuc-II have been given in Table-I of the subsection 2.1 above.

3.2. Constraints on the DM models

In this subsection, we have fitted the possible γ -ray flux from Tuc-II in terms of the flux arising out of the pair-annihilation of the WIMPs by employing a full-scale MC simulation package DMFit [37, 49], as implemented in the

ScienceTools. The DMFit package is based on the particular set of MC simulations of hadronization and/or decay of the annihilation products as used by the DarkSUSY team [37, 49] by means of the Pythia 6.154 [50] event generator. With that package, we have first fitted the LAT-observed γ -signal from Tuc-II with an estimated 95% C.L. γ -flux upper limits as described in subsection 2.2 of this paper. By employing the DMFit package, we could also determine the variation of the thermally averaged pair-annihilation $\langle \sigma v \rangle$ of the WIMPs with the variation of the plausible WIMP masses (m_{DM}), for various important pair-annihilation final states (f), i.e. for each of the possible important channels in which WIMP annihilations might take place to produce γ -rays. For the purpose of this paper, we have considered five such supersymmetry-motivated pair annihilation final states [7], namely 100% $b\bar{b}$, 80% $b\bar{b}$ +20% $\tau^+\tau^-$, the 100% $\tau^+\tau^-$, 100% $\mu^+\mu^-$ and 100% W^+W^- , respectively. The variation of such 95% C.L. γ -flux upper limits and of their corresponding annihilation $\langle \sigma v \rangle$ with increasing WIMP masses are displayed in Fig. 2(a,b), separately for each of the annihilation channels mentioned above.

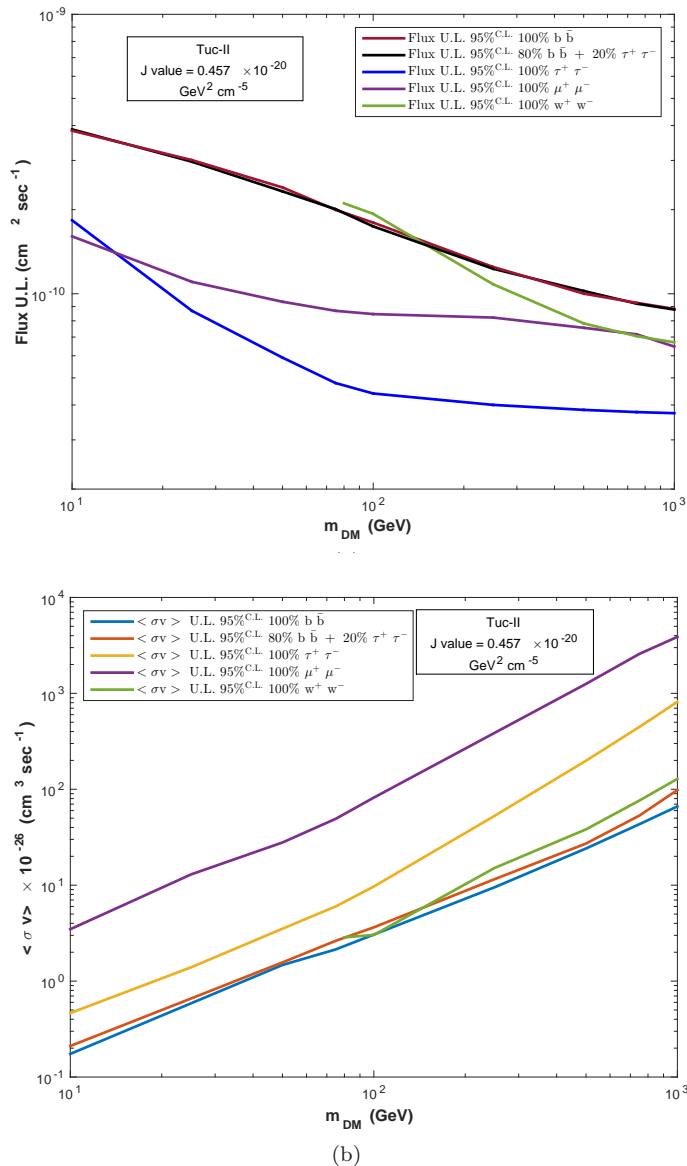


FIG. 2: Variations of (a) the 95% C.L. γ -ray (integral) flux upper limits and of (b) the corresponding pair-annihilation $\langle \sigma v \rangle$ of the WIMPs with their increasing masses (m_{DM}), as estimated for various annihilation final states “f” (indicated in the diagram) by using the DMFit package.

In Figs. 3(a,b) and 4, we have displayed the DMFit-determined 95% C.L. upper limit of the thermally averaged WIMP pair-annihilation $\langle \sigma v \rangle$, as a function of the WIMP mass (m_{DM}), as obtained from the analysis of LAT-data in

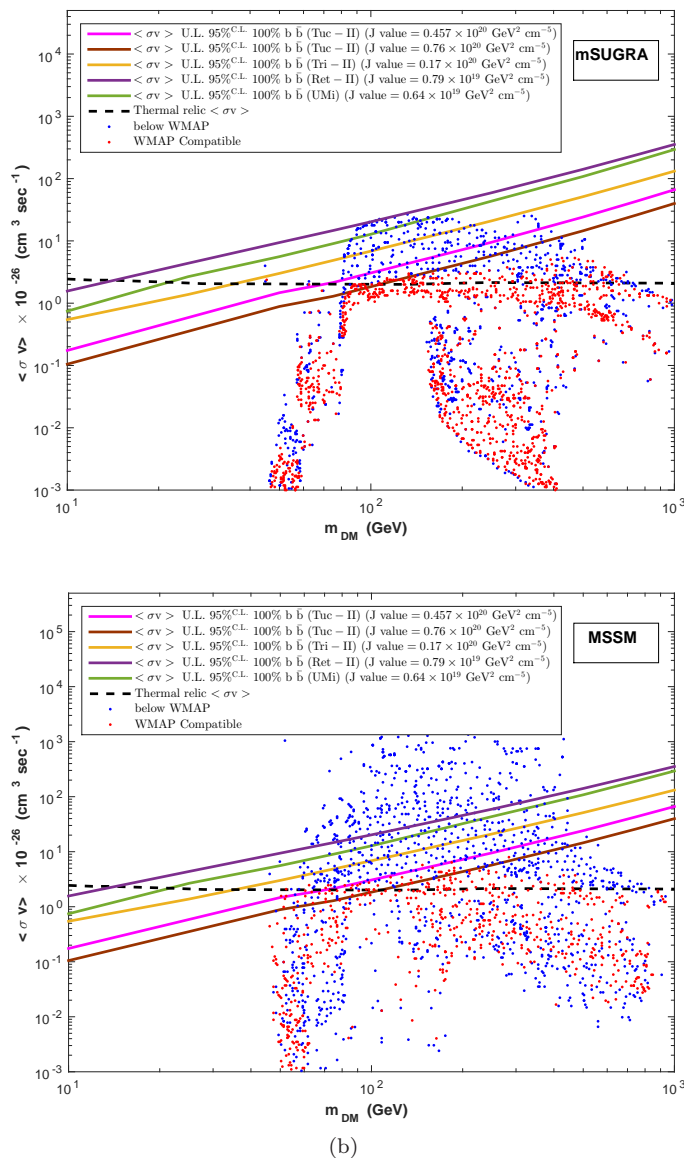


FIG. 3: Variation of 95% C.L. upper limit of the WIMP pair-annihilation $\langle \sigma v \rangle$ with increasing m_{DM} for only the $b\bar{b}$ annihilation final states in Tuc-II displayed in $(m_{\text{WIMP}}, \langle \sigma v \rangle)$ plane for two J values, namely the value obtained from Eq. (4) (represented by the pink line) and the one obtained in Ref. [39] by using an analytical integration of Eq. (3) for NFW model under certain assumptions (represented by the brown line). In the figures, the $\langle \sigma v \rangle$ are compared with points derived from (a) the mSUGRA and of (b) the MSSM models [5]. In those later models, the red points correspond to thermal relic density compatible with the WIMP data. The blue points represent higher $\langle \sigma v \rangle$, and correspondingly lower thermal relic densities, obtained by assuming certain additional nonthermal production mechanisms to contribute to WIMP production, while the WIMPs still comprise all of the dark matter. In both the figures, the dark, broken-dashed line represents $\langle \sigma v \rangle$ of any mass required to reproduce the observed DM density of our universe. In these figures, we have also overlotted the the *Fermi*-obtained 95% C.L. upper limits of the annihilation $\langle \sigma v \rangle$ for three UFDs, namely, Tri-II, UMi and Ret-II, represented by the yellow, green and the magenta lines, respectively. For Tri-II, we have used the J -value obtained in Paper-I, while for UMi and Ret-II, we have used the J -values obtained in Refs. [5] and [24], respectively.

the direction of Tuc-II, for two different values of J , namely, $0.457 \times 10^{20}(\text{GeV}^2\text{cm}^{-5})$ and $0.76 \times 10^{20}(\text{GeV}^2\text{cm}^{-5})$. $0.457 \times 10^{20}(\text{GeV}^2\text{cm}^{-5})$ is obtained by using Eq. (3) and the other value is obtained from Ref. [39]. These results are then compared with the $\langle \sigma v \rangle$ values obtained for various WIMP masses (m_{DM}) from four theoretical DM models, namely the minimal Supergravity (mSUGRA; in Fig. 3(a)) [51] model, the Minimal Supersymmetric Standard Model (MSSM; in Fig. 3(b)) [52] model, the Anomaly Mediated Supersymmetry Breaking model (AMSB) [53] (in Fig. 4) model and the lightest Kaluza-Klein particle of Universal Extra Dimensions (UED) model[54–56] (in Fig. 4),

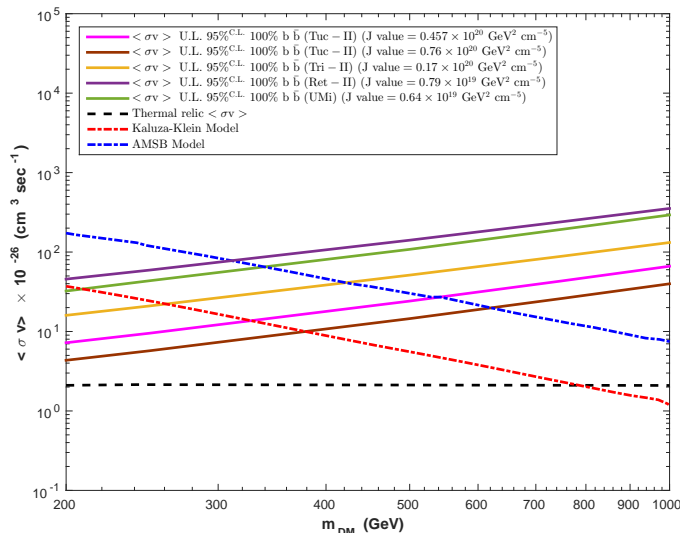


FIG. 4: A comparison between the DMFit-obtained 95% C.L. upper limit of $\langle \sigma v \rangle$ vs. m_{DM} curve from Tuc-II and the theoretical $\langle \sigma v \rangle$ vs. m_{DM} curves obtained from the AMSB and the Kaluza-Klein UED models only for $b\bar{b}$ annihilation channel. As in Figs. 3(a,b), we overplot the results from Tri-II, UMi and Ret-II in this figure also. The colors and the line-styles of different curves are indicated in the diagram.

respectively. Only the annihilation $\langle \sigma v \rangle$ in 100% $b\bar{b}$ channel has been considered in these figures as they are found to put the most stringent limits on the parameter space of the models. In Figs. 3(a,b) and 4, we also overplot the 95% C.L. upper limit of the WIMP annihilation $\langle \sigma v \rangle$ obtained by the analysis of nine years of LAT-data in the directions of three other UFDs, namely Tri-II, UMi and Ret-II, respectively. The J value used to analyse Tri-II data has been obtained by using Eq. (3); cf. Paper-I. For UMi and Ret-II, on the other hand, we have straightway used the J values determined (for UMi) in Ref. [5] and (for Ret-II) in Ref. [24], respectively. The results for Tri-II and UMi that are displayed in Figs. 3(a,b) and 4, are in good agreement with the earlier results presented in Paper I (for both Tri-II and UMi) and in Ref. [5] (for UMi alone), respectively. It may also be of some interest to note that, in their recent analysis of the *Fermi*-data, the *Fermi*-DES collaboration [24] has detected slight excess in γ -emission of 2.3σ significance, for a WIMP mass $m_{\text{DM}} = 15.8$ GeV, in the direction of Ret-II. This is in general agreement with our results, in which we also obtain an excess of $\approx 2\sigma$ significance for similar WIMP masses in the case of Ret-II.

From the Figs. 3 and 4, it is immediately evident that Tuc-II imposes comparatively tighter constraint on the parameter spaces of the popular theoretical WIMP models than the ones imposed by Ret-II, UMi, and even by Tri-II. The last one was shown to be a particularly good candidate for constraining the DM models in Paper-I. In Fig. 3(b), it is interesting to note that, even with a somewhat worse J value (obtained by using Eq. (3)) of Tuc-II, the upper limit of $\langle \sigma v \rangle$ values have already begun to constrain those MSSM model points (in red color) that are consistent with the cosmological thermal relic density, while in Fig. 3(a), they considerably constrain only the blue points, representing low thermal relic density but additional nonthermal production mechanisms for the WIMPs, in the case of the mSUGRA model. For a higher J value, Tuc-II constrains the red points in mSUGRA as well. This is unlike the cases for UMi, Ret-II and Tri-II that constrain only the blue points in both the mSUGRA and the MSSM models. It is also to be noted that, at about 100 GeV WIMP mass, the upper limit of $\langle \sigma v \rangle$ for Tuc-II is lowered by factors of 2, 6 and 4 than the corresponding upper limits in the cases of Tri-II, Ret-II and UMi respectively. Fig. 4 shows that the upper limit of $\langle \sigma v \rangle$ from Tuc-II (with $J = 0.457 \times 10^{20} \text{ GeV}^2 \text{ cm}^{-5}$, as determined from Eq. (3) above) disfavors the AMSB and the Kaluza-Klein UED models for masses < 550 GeV and < 350 GeV respectively, while, Tri-II Ret-II and UMi allow lower WIMP masses with respect to those theoretical models displayed in Fig. 4. For a higher J value of Tuc-II, $J = 0.76 \times 10^{20} \text{ GeV}^2 \text{ cm}^{-5}$, on the other hand, Fig. 4 disfavors the Kaluza-Klein UED and the AMSB model for masses below < 650 GeV and < 400 GeV, respectively.

4. CONCLUSIONS AND DISCUSSION

In this paper, we have analysed nearly nine years of *Fermi*-LAT γ -ray data from one of the recently discovered UFDs, namely Tuc-II, with the purpose of detecting the signatures of self-annihilation of the WIMPs that are usually believed to be the constituent particles of DM within the UFDs/dSphs. No significant γ -ray emission above 100 MeV

has, however, been detected from Tuc-II in this study. We have, therefore, determined the 95% C.L. upper limit of the γ -ray flux from Tuc-II that might arise from the pair-annihilation of the WIMPs in Tuc-II. This upper-limit has been obtained by fitting *Fermi*-data-points from Tuc-II with the fluxes simulated by using the DMFit MC simulation package for in a quasi-model independent manner. By using Eq. (2), we could then determine the possible upper-limit of the pair-annihilation $\langle \sigma v \rangle$ of the WIMPs in Tuc-II, as the function of WIMP mass, in each of the annihilation channels considered here with an assumption that the entire γ -ray emission arises for particle interaction in that channel only. In this paper, we find that, even with a moderate value of the J -factor determined from an approximate, analytical expression given earlier in the literature, our results could impose more stringent constraints on the theoretical WIMP annihilation $\langle \sigma v \rangle$ obtained in the popular WIMP models than the similar constraints imposed by the observed data from other known dSphs/UFDs, namely the UMi, Tri-II and Ret-II that have earlier been considered in the literature to be the good candidates for the search of DM. Our study, presented in this paper, further reveals that we can, in fact, get even better constraints on the theoretical models with a slightly enhanced J value for Tuc-II, as obtained from an exact analytical solution of the spherical Jeans' equation, as applied to the NFW profile alone for the DM.

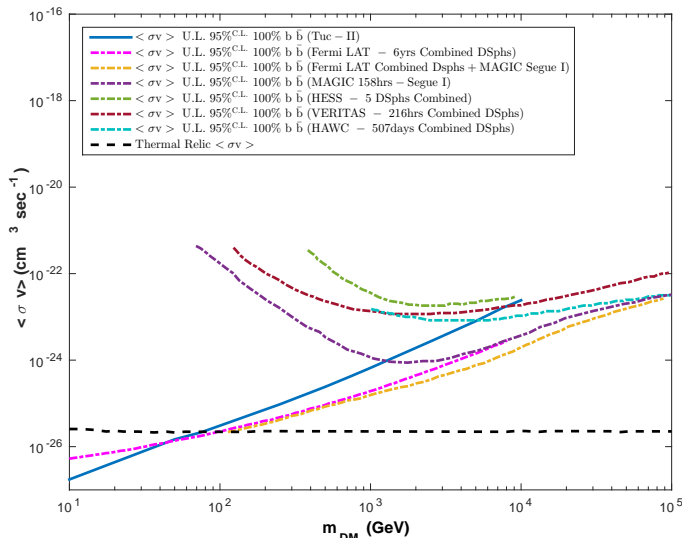


FIG. 5: $\langle \sigma v \rangle$ vs. m_{DM} for $b\bar{b}$ annihilation channel from Tuc-II (obtained in this paper) is shown in comparison with the results obtained from single or combined dSph studies by HESS([59]), HAWC([60]), VERITAS([61]), MAGIC([58]), *Fermi*-LAT([57]) and *Fermi*-LAT+MAGIC([58]) groups, respectively.

In this final section of the paper, we would like to make a comparative study of the upper limits of WIMP pair-annihilation $\langle \sigma v \rangle$, as obtained in this paper, with the $\langle \sigma v \rangle$ obtained from other studies of the dSphs/UFDs. This comparison is displayed in Fig. 5. It includes the results obtained from a combined analysis [57] of 15 dSphs from six years of *Fermi*-LAT data, the results from an analysis [58] of γ -ray data from Segue-I, obtained earlier by using the Major Atmospheric Gamma-ray Imaging Cherenkov Telescopes (MAGIC) alone, as well as, the ones obtained from Segue-I by a joint *Fermi*+MAGIC [58] collaboration. Fig 5 also includes the results from the analysis [59] of data from a combined study of 5 dSphs by the High Energy Stereoscopic System (H.E.S.S.) of IACT telescopes and the results from the combined study of 15 dSphs [60] by the High Altitude Water Cherenkov (HAWC) gamma ray observatory and of 4 dSphs [61] by the Very Energetic Radiation Imaging Telescope Array System (VERITAS), as well. In Fig. 5, we find that the joint *Fermi*+MAGIC observations of Segue-I puts the best overall limit on the DM annihilation $\langle \sigma v \rangle$ for a wide range of WIMP masses than the limits obtained by various other observations incorporated in that figure. As expected, the combined dSph analysis by the *Fermi*-group also fares well at masses upto about 1 TeV, above which the *Fermi*-LAT begins to have low statistics. The comparison displayed in Fig. 5 seems to conform to the intuitive belief that the Cherenkov detector arrays should impose stringent limits on the annihilation $\langle \sigma v \rangle$ in the mass range $\gtrsim 10$ TeV, while a joint analysis of spaced based + ground based detector is likely to impose most stringent limits on $\langle \sigma v \rangle$ in the mass range $\lesssim 1$ TeV. It might be interesting to note that, the upper-limits on $\langle \sigma v \rangle$ obtained by HAWC and by the *Fermi*+MAGIC groups tend to converge in the mass range ≈ 100 TeV, which might indicate that both the IACTs and the Water Cherenkov detectors are becoming competitive in regards to the DM search in the dSphs/UFDs. However, the limiting $\langle \sigma v \rangle$, displayed in Fig. 5, at $\lesssim 1$ TeV WIMP mass range is still about two orders of magnitude away from its relic abundance value. A coordinated effort to combine the data taken from several γ -ray telescopes, as well as, the enhancements of the sensitivity of the Cherenkov

telescopes and the improvements of the data analysis techniques of the γ -ray telescopes in general seem, therefore, to be the pressing necessities.

Acknowledgement

PB is grateful to DST INSPIRE Fellowship Scheme for providing the support for her research. We would like to thank Dr. Stefano Profumo and Dr. Tesla Jeltema of University of California, Santa Cruz, U.S.A., for providing useful guidance in Fermi-LAT data analysis. We are particularly grateful to the *Fermi* Science Tools for allowing us to freely access the *Fermi*-LAT data and providing all the needed guidance for our analysis.

-
- [1] E. Komatsu *et al.*, *Astrophys. J. Suppl.* **192**, 18 (2011).
 - [2] P. A. R. Ade *et al.* [Planck Collaboration], *Astron. and Astrophys.* **594**, A13 (2016).
 - [3] J. Diemand *et al.*, *Nature*, **454**, 735 (2008).
 - [4] V. Springel *et al.*, *MNRAS*, **391**, 1685 (2008).
 - [5] A. A. Abdo *et al.*, *Astrophys. J.* **712**, 147 (2010).
 - [6] G. Steigman and M. S. Turner, *Nucl. Phys. B.* **253**, 375 (1985); G. Bertone, D. Hooper and J. Silk, *Phys. Rept.* **405**, 279 (2005).
 - [7] G. Jungman, M. Kamionkowski and K. Griest, *Phys. Rep.* **267**, 195 (1996).
 - [8] A. W. McConnachie, *Astron. J.* **144**, 4 (2012).
 - [9] S. Piatek *et al.*, *Astrophys. J.*, **124**, 3198 (2002).
 - [10] E.K.Grebel *et al.*, *Astron. J.* **125**, 4 (2003).
 - [11] D. G. York *et al.*, *Astron. J.* **120**, 1579 (2000).
 - [12] V. Belokurov *et al.*, *Astrophys. J.* **712**, L103 (2010).
 - [13] N. Kaiser *et al.*, Conference on Survey and Other Telescope Technologies and Discoveries, Waikoloa, Hawaii, August 27-28, (2002), *Proc. SPIE. Int. Soc. OPT. Eng.* **4836**, 154 (2002).
 - [14] B. P. M. Laevens *et al.*, *Astrophys. J.* **813**, 44 (2015).
 - [15] B. P. M. Laevens *et al.*, *Astrophys. J. Lett.* **802**, L18 (2015).
 - [16] T. Abbott *et al.* [Dark Energy Survey], arXiv: 0510346v1 (2005).
 - [17] K. Bechtol *et al.* [Dark Energy Survey], *Astrophys. J.* **807**, 50 (2015).
 - [18] S. E. Kogosov *et al.*, *Astrophys. J.* **805**, 130 (2015).
 - [19] D. Kim and H. Jerjen, *Astrophys. J. Lett.* **808**, L39 (2015).
 - [20] D. Kim *et al.*, *Astrophys. J. Lett.* **804**, L44 (2015).
 - [21] N. F. Martin *et al.*, *Astrophys. J. Lett.* **804**, L5 (2015).
 - [22] A. Koch *et al.*, *E Phys. J. web of conferences* **19**, 03002 (2012).
 - [23] D. Kim, Search for Ultra-Faint Milky Way Satellites, *Ph.D Thesis*, Australian National University, 2017.
 - [24] A. Albert *et al.*, *Astrophys. J.* **834**, 110 (2017).
 - [25] M. Ackermann *et al.*, *Phys. Rev. Lett.* **115**, 231301 (2015).
 - [26] C. He *et al.*, *Phys. Rev. D*, **91**, 063515 (2015).
 - [27] Sayan Biswas *et al.* *J. Cosmol. Astropart. Phys.* **11**, 003 (2017).
 - [28] M. G. Walker *et al.*, *Astrophys. J.* **819**, 53 (2016).
 - [29] G. Gilmore *et al.*, *Nucl. Phys. B.* **173**, 15 (2007)
 - [30] E. N. Kirby *et al.*, *Astrophys. J.* **779**, 102 (2013).
 - [31] M. L. Mateo, *Astron. and Astrophys.* **36**, 435 (1998); J. S. Gallagher *et al.*, *Astrophys. J.* **588**, 326 (2003); J. Grevious and M. E. Putman, *Astrophys. J.* **696**, 385 (2009).
 - [32] A. P. Ji *et al.*, *Astrophys. J. Lett.* **832**, L3 (2016).
 - [33] N. F. Martin *et al.*, *Astrophys. J.* **864**, 1075 (2008).
 - [34] R. R. Munoz *et al.*, *Astron. J.* **140**, 138 (2010). (2013).
 - [35] S.E. Kogosov *et al.*, *Astrophys. J.* **811**, 62 (2015).
 - [36] A. Geringer-Sameth, S.M. Koushiappas and M. Walker, *Astrophys. J.* **801**, 74 (2015).
 - [37] T. E. Jeltema and S. Profuma, *J. Cosmol. Astropart. Phys.* **11**, 003 (2008).
 - [38] A. Drilica-Wagner *et al.* (DES-collaboration), *Astrophys. J.* **813**, 109 (2015).
 - [39] N. W. Evans, J. L. Sanders, A. Geringer-Sameth, *Phys. Rev. D* **93**, 103512 (2016).
 - [40] M.G. Walker *et al.*, *Astrophys. J.* **704**, 1274 (2009).
 - [41] J. Wolf *et al.* *MNRAS*, **406**, 1220 (2010).
 - [42] W. Cash, *Astrophys. J.* **228**, 939 (1979).
 - [43] J. R. Mattox, *et al.*, *Astrophys. J.* **461**, 396 (1996).
 - [44] F. Acero, *et al.*, *Astrophys. J. Suupl.* **218**, 23 (2015).
 - [45] W. Rolke, A. Lopez, J. Conrad, *Nucl. Instrum. Methods A*, **551**, 493 (2005).

- [46] R. Barbieri, S. Ferrara and C. A. Savoy, *Phys. Lett. B* **119**, 343 (1982).
- [47] E. A. Baltz *et al.*, *J. Cosmol. Astropart. Phys.* **07**, 13 (2008).
- [48] J. F. Navarro, C. S. Frenk, S. D. M. White, *Astrophys. J.* **490**, 493 (1997).
- [49] P. Gondolo *et al.*, *J. Cosmo Astropart. Phys.* **07**, 008 (2004).
- [50] T. Sjostrand, S. Mrenna, P.Z. Skands, *Comput. Phys. Commun.* **178**, 852 (2008).
- [51] A. H. Chamseddine, R. Arnowitt, P. Nath, *Phys. Rev. Lett.* **49**, 970 (1982).
- [52] D. J. H. Chung *et al.*, *Phys. Rep.* **407**, 1 (2005).
- [53] G. F. Giudice, R. Rattazi, M. A. Luty and H. Murayama, *J. High Energy Phys.* **12**, 027 (1998); L. Randall and R. Sundrum, *Nucl. Phys. B* **557**, 79 (1999).
- [54] H. C. Cheng, J. L. Feng, K. T. Matchev, *Phys. Rev. Lett.* **89**, 211301 (2002).
- [55] G. Servant and T. M. P. Tait, *Nucl. Phys. B* **650**, 391 (2003).
- [56] D. Hooper and S. Profumo, *Phys. Rep.* **453**, 29 (2007).
- [57] [Fermi-LAT Collaboration] M. Ackerman *et al.*, *Phys. Rev. Lett.* **115**, 231301 (2015).
- [58] [MAGIC Collaboration] M. L. Ahnen *et al.*, *J. Cosmol. Astropart. Phys.* **2**, 039 (2016).
- [59] [HESS Collaboration] A. Abramowski *et al.*, *Phys. Rev. D* **90**, 112012 (2014).
- [60] [HAWC Collaboration] M. L. Proper *et al.*, ICRC,**LA-UR-15-25701**, 0402 (2015).
- [61] [VERITAS Collaboration] S. Archambaut *et al.*, *Phys. Rev. D* **95**, 082001 (2017).